Hindawi
Journal of Spectroscopy
Volume 2021, Article ID 6677219, 10 pages
https://doi.org/10.1155/2021/6677219

Research Article

Species Identification and Effects of Aromatic Hydrocarbons on the Fluorescence Spectra of Different Oil Samples in Seawater

Yongchao Hou,[1] Ying Li,[1,2] Guannan Li,[1] Mingfei Xu,[1] and Yunpeng Jia[1]

[1]*Navigation College, Dalian Maritime University, Dalian 116026, China*
[2]*Environmental Information Institute, Dalian Maritime University, Dalian 116026, China*

Correspondence should be addressed to Ying Li; hyc@dlmu.edu.cn

Received 29 December 2020; Revised 18 February 2021; Accepted 17 March 2021; Published 27 March 2021

Academic Editor: Jose S. Camara

The identification of oil species and their characteristics in oil spills is particularly important for their efficient disposal. Since aromatic hydrocarbons (AHs) with various characteristics are the major fluorescent components of oils in seawater, they can be used to detect different oil species in seawater. Here, we developed a composition method using the fluorescence spectra of eight AH categories analyzed by gas chromatography-mass spectrometry (GC-MS) to evaluate the contribution of AHs to the total fluorescence of six different oil species. Qualitative and quantitative difference analysis of the experimental and composite fluorescence spectra was performed based on the redshift of the main peak position, the fluorescence intensity distance, and the generalized included angle cosine, while correlation analysis was used to establish the relationship between the different fluorescence spectral parameters and the American Petroleum Institute gravity and viscosity of the oil species. The fluorescence spectra recorded for heavy oil samples indicated a reduction in the fluorescence signal of fluorene series and an increase in the contribution of acenaphthene and pyrene series, indicating that the currently developed composition method by fluorescence spectroscopy combined with GC-MS can be used to distinguish and identify oil species in seawater samples.

1. Introduction

Oil spills are one of the most common contaminants in marine environments that seriously affect all aspects of marine ecology and transport [1, 2]. Early determination and characterization of oil spills in terms of oil species, oil film thickness, and oil distribution can significantly facilitate decision-making for effective emergency disposal and cleanup programs [3, 4]. To date, remote sensing techniques, such as microwave, infrared, fluorescence, and visible remote sensing, as well as chemical analytical methods, including gas or liquid chromatography coupled with mass spectrometry (GC-MS or LC-MS), have been most frequently used to detect oil slicks and identify oil species in seawater [5–7].

Fluorescence spectroscopy is a useful diagnostic tool used to evaluate petroleum hydrocarbons in natural seawater either separated by extraction and fractionation or not separated using direct detection methods [8, 9]. Most petroleum products emit light at longer wavelengths than the excitation light on their own or in organic solvents, as they consist of aromatic hydrocarbons (AHs) that have aromatic structures and bear conjugated double bonds with intrinsic fluorescence properties in the ultraviolet-visible (UV-vis) region (Figure 1) [10, 11]. Furthermore, AHs are the major fluorescent components in petroleum and predominate in the fluorescence spectra of sea surface oil slicks [12–14]. Thus, petroleum products containing different AH groups exhibit different fluorescence characteristics, which have been recently used to successfully detect and identify oil species in seawater [15, 16]. In addition, the development of reliable and relatively inexpensive instruments by fluorescence spectroscopy has enabled real-time detection of petroleum hydrocarbons, identification of oil species, and measurement of oil thickness in oil slicks [17–19].

Due to their carcinogenic and toxic properties, AHs can be easily transferred and accumulated in food chains, thereby harming living organisms [20]. Fluorescence

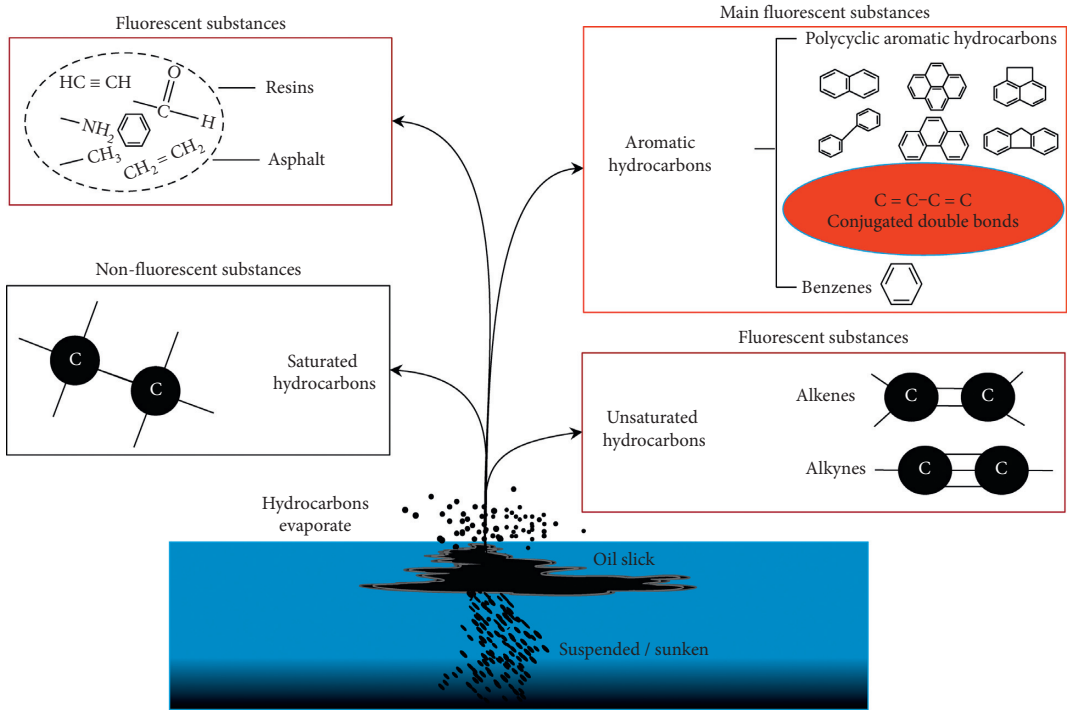

Figure 1: Fluorescent and nonfluorescent substances found in oil slicks.

spectroscopy has been employed to analyze AHs in the marine environment [21, 22], while several studies have used GC-MS and stable isotope analysis to distinguish and quantify the AH content in petroleum-based products such as diesel, fuel, and crude oils [23–25]. In addition, the United States Environmental Protection Agency (US-EPA) has indicated a number of AHs as priority pollutants and summarized some of their key photophysical properties, which reflect their absorption and fluorescence behavior on sea surface or in seawater [26]. It has been reported that the presence of AHs in different oil species can significantly affect their fluorescence spectra, as they can generate characteristic fluorescence emissions [27]. However, the analyses of relationship between the chemical components and fluorescence spectra of different oils are yet to be developed. Therefore, the effect of AHs on the fluorescence spectra of oil species should be particularly considered during qualitative and quantitative analysis, especially when fluorescence spectroscopy is used to accurately distinguish oil species. To the best of our knowledge, the fluorescence spectroscopy method has never been applied to analyze the contribution of AHs fluorescence to the fluorescence spectra of different oils; we believe that this method can better detect and identify oil species.

Here, we studied the effects of AHs on the fluorescence spectra of crude, fuel, and diesel oil seawater samples. To that end, we established a composition method using the fluorescence spectra of individual AHs bearing 2–4 rings to evaluate their contribution to the fluorescence spectra of the different oil species. More specifically, the relative content of each AH in each sample was measured by GC-MS, and the fluorescence spectroscopic data of the individual AHs were obtained from the US-EPA. In addition, the fluorescence spectra of the oil samples were recorded using a spectrofluorometer, and the differences between the experimental and composite fluorescence spectra were evaluated based on the spectral intensity and overall shape characteristics. The ultimate goal of this study was to assess the relevance of the relative content of AHs in the detection and identification of oil species in seawater based on their fluorescence signatures.

2. Materials and Methods

2.1. Oil Samples. Seawater samples were collected in October 2020 at the port of Lingshui, northern Yellow Sea, China. Kuwait and Iranian crude oil, 380# and 180# fuel oil, and 0# and −10# diesel oil samples were used as representatives of light crude oil, heavy fuel oil, and refined oil (diesel), respectively (Table 1). For laboratory measurements, small amounts of the oil samples were weighed, added to a seawater sample, and shaken vigorously to reach the desired oil concentration in seawater (0.02 mg/L).

The fluorescence emission spectra of the samples were measured using a Cary Eclipse Varian spectrofluorometer using a 1 × 1 cm quartz cuvette. The fluorescence wavelength ranged between 260 and 700 nm with a 5 nm emission sampling interval, a 10 nm excitation slit, and a 10 nm emission slit. An excitation wavelength of 266 nm was selected to measure the fluorescence emission, as it was in the range where oil samples show high absorption and corresponded to a typical excitation wavelength of a Nd : YAG laser used for laser-induced fluorescence measurements applied directly in oil spill detection [28, 29].

Table 1: Characteristics of the tested oil samples.

Number	Oil sample	API gravity[1] (°)	Viscosity (50°C, mm^2/s)	Oil species
1	Kuwait crude	31.8	6.96	Light crude oil
2	Iranian crude	35.0	5.2	Light crude oil
3	180# fuel	11.3	180.0	Heavy fuel oil
4	380# fuel	11.3	380.0	Heavy fuel oil
5	0# diesel	38.2	3.35	Refined oil
6	−10# diesel	38.2	3.40	Refined oil

[1]American Petroleum Institute (API) gravity = (141.5/specific gravity (60°F))−131.5.

2.2. GC-MS Analysis. The content of AHs in oil samples was analyzed based on our previous GC-MS studies [30, 31]. Each oil sample (~0.2 g) was weighed and dissolved in 8 mL *n*-hexane, and the aromatics were fractionated using a chromatographic column (0.47 cm i.d. × 12 cm). The column was dry-packed with 3 g of silica gel (activated at 180°C for 20 h, 100–200 mesh, AR) and was topped with about 1 cm anhydrous sodium sulfate (activated at 350°C for 4 h, AR). The column was eluted with hexane, and the eluent was discarded before exposing the sodium sulfate layer to air. Approximately 200 μL of the concentrated extract was quantitatively transferred for GC-MS analysis. The aromatics were eluted with *n*-hexane/dichloromethane mixture (15 mL, 1 : 1 v/v) and concentrated to 1 mL under N_2 flow prior to GC-MS analysis. GC-MS (Thermo Fisher Scientific, Waltham, MA, USA) was performed such that 1 μL of each sample was injected in a DB-5MS quartz chromatographic column (60 m × 0.25 mm × 0.25 μm) in the splitless mode. The GC temperature program involved heating from 60°C to 100°C at a rate of 20°C/min, where it was maintained for 6 min. Then, the temperature was increased from 100°C to 300°C at 4°C/min and isothermally maintained at 300°C for 35 min. For the MS measurements, the injector, interface, and ion source were maintained at 280°C, 250°C, and 200°C, respectively. The electron bombardment source for electron impact was 70 eV.

2.3. Fluorescence Composition Method. A fluorescence composition method was developed using the fluorescence spectra of individual AHs to evaluate their contribution to the total fluorescence of the oil samples. Moreover, the sum of these contributions was used to prepare a composite spectrum, which was further used to determine the total contribution of AHs bearing 2–4 rings to the fluorescence of different oil species following already reported studies [32, 33]. The fluorescence composition method of the identified AHs could be expressed in matrix/vector notation as follows:

$$\mathbf{I}_f^{\text{oil}} = \mathbf{I}_f^{\text{AH}} \mathbf{X}_F \mathbf{X}_C, \quad (1)$$

where $\mathbf{I}_f^{\text{oil}}$ is the $n_\lambda \times 1$ vector of the computed or measured fluorescence intensity (n_λ = number of wavelengths between 260 and 700 nm), $\mathbf{I}_f^{\text{AH}}$ is the $n_\lambda \times n_{\text{AH}}$ matrix of the AH fluorescence based on the fluorescence spectra data obtained from the US-EPA (n_{AH} = number of AHs), $\mathbf{X_F}$ is the $n_{\text{AH}} \times n_{\text{AH}}$ diagonal matrix representing the contribution rate of each AH to the total fluorescence spectra (when $\mathbf{X_F} = \mathbf{E}$ obtaining the composite spectrum, $\mathbf{E}$ is the identity matrix), and $\mathbf{X_C}$ is the $n_{\text{AH}} \times 1$ vector of the relative content of each AH (determined by GC-MS) in the total identified AHs extracted from each oil sample.

3. Results and Discussion

3.1. Distribution and Categories of AHs. The relative content of AHs in Kuwait crude, Iranian crude, 380# fuel, 180# fuel, 0# diesel, and −10# diesel oil samples was determined by GC-MS after extraction and fractionation (Figure 2), and the types of AHs included in each oil sample were identified by matching the retention times to 16 standard AHs [34, 35]. Specifically, the AHs detected in the six oil samples were naphthalene, methylnaphthalene, dimethylnaphthalene, trimethylnaphthalene, biphenyl, methylbiphenyl, 2, 2' + 4, 4'-dimethylbiphenyl, acenaphthene, fluorene, methylfluorene, dibenzothiophene, methyldibenzothiophene, 2, 4 + 4, 6-dimethyldibenzothiophene, phenanthrene, methylphenanthrene, dimethylphenanthrene, trimethylphenanthrene, pyrene, methylpyrene, and chrysene. The AH contents in the oil samples were determined by analyzing a standard mixture containing known concentrations of each AH. Moreover, the alkyl aromatic hydrocarbon compounds were identified by comparing the mass spectra and retention times obtained in this study with existing data [36, 37].

Petroleum, a complex mixture containing multiple fluorescent substances, and the differences in photophysical properties and content of each component affect the overall fluorescence characteristics and intensity of the oil samples in seawater. It is, therefore, clear that the composition of the oil samples in AHs is complex, making it difficult to analyze the effect of the individual ingredients on the fluorescence spectra. Moreover, the effect of alkane substituents on the fluorescence spectra is generally weak, suggesting that AHs bearing alkyl substituents would exhibit similar fluorescence spectra [38, 39]. Therefore, AHs were divided into eight categories, namely, naphthalene, biphenyl, acenaphthene, fluorene, dibenzothiophene, phenanthrene, pyrene, and chrysene series (Table 2). Dominant AHs with a relative content of 60.88%, 60.90%, and 65.93% in Kuwait crude oil, Iranian crude oil, and 180# fuel oil, respectively, belonged to the naphthalene series. In contrast, the AHs in 380# fuel oil were almost equally distributed, and the highest contents were detected in the naphthalene (33.15%), dibenzothiophene (16.85%), and phenanthrene series (27.46%). Furthermore, the diesel oil samples included mainly AHs with

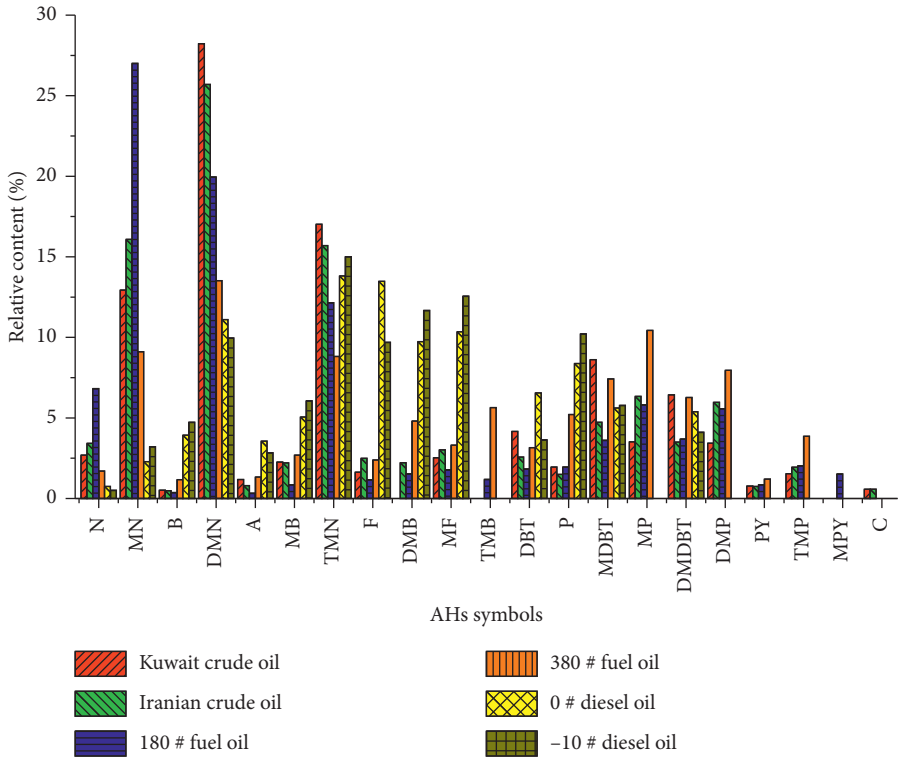

Figure 2: Relative content of AHs in six oil samples determined by GC-MS analysis. Naphthalene (N); methylnaphthalene (MN); dimethylnaphthalene (DMN); trimethylnaphthalene (TMN); biphenyl (B); methylbiphenyl (MB); dimethylbiphenyl (DMB); acenaphthene (A); fluorene (F); methylfluorene (MF); dibenzothiophene (DBT); methyldibenzothiophene (MDBT); dimethyldibenzothiophene (DMDBT); phenanthrene (P); methylphenanthrene (MP); dimethylphenanthrene (DMP); trimethylphenanthrene (TMP); pyrene (PY); methylpyrene (MPY); and chrysene (C).

two or three benzene rings. Hence, the relative contents of the eight AH categories in the six oil samples were used as the values of the $\mathbf{X_C}$ parameter in the fluorescence composition method with $n_{\mathrm{AH}} = 8$.

3.2. Composite and Experimental Fluorescence Spectra. To analyze the fluorescence contribution of AHs, the composite fluorescence spectra of the six oil samples were determined using equation (1) based on the fluorescence spectra of the individual AHs obtained from the US-EPA, which were distributed over a wavelength range of 285–525 nm with a resolution of 1 nm (Figure 3). Hence, the $n_\lambda \times n_{\mathrm{AH}}$ matrix of the individual AHs fluorescence spectra represented the $\mathbf{I}_f^{\mathrm{AH}}$ parameter in the composition method with $n_\lambda = 241$ and $n_{\mathrm{AH}} = 8$. Moreover, due to the unknown contribution of the individual AHs to the fluorescence spectra of the oil samples, $\mathbf{X_F}$ was calculated as a 8×8 identity matrix (equation (2)) to obtain the composite fluorescence spectra *via* the composition method. As shown in Figure 4(a), the composite fluorescence spectra of all oil samples exhibited one main peak, which ranged between 320 and 350 nm and was centered at 330 nm. However, the fluorescence intensity of the 380# fuel oil composite between 350 and 450 nm was higher compared to the other oil samples and exhibited several small peaks in this wavelength range. Moreover, the fluorescence intensity of the 0# and −10# diesel oil composites in the 300–320 nm region was higher than that of the other oil samples. These results were used as comparative data to analyze the differences of the experimental fluorescence spectra and verify the contribution of different AHs to the fluorescence of the examined oil samples.

$$\mathbf{X_F} = \mathbf{E} = \begin{bmatrix} 1 & 0 & \dots & 0 \\ 0 & 1 & \dots & 0 \\ \vdots & \vdots & \ddots & \vdots \\ 1 & 0 & \dots & 1 \end{bmatrix}_{8\times 8}. \quad (2)$$

The experimental fluorescence spectra of the six oil samples were recorded using UV-excited (λexc = 266 nm) and normalization and adjacent average smoothing to eliminate environmental and instrumental errors during the measurement process (Figure 4(b)) [40]. The experimental spectra were then directly compared with the respective composite fluorescence spectra of the six oil samples at a wavelength range of 285–525 nm, to better understand the effects of AHs on the fluorescence of oil seawater samples (Figure 4(c)). As shown in Figure 4(c), the experimental spectra were redshifted compared to the composite fluorescence spectra and exhibited significant fluorescence intensity in the long-wavelength region (350–500 nm). Moreover, the experimental fluorescence spectra of the crude and diesel oil were very similar to the respective composite spectra. In contrast, great deviations were observed for the 380# and 180# fuel oil samples, while the small

Table 2: Relative content of eight AH categories in Kuwait crude, Iranian crude, 380# fuel, 180# fuel, 0# diesel, and −10# diesel oil samples.

AHs[a]	Categories	Kuwait crude (%)	Iranian crude (%)	180# fuel (%)	380# fuel (%)	0# diesel (%)	−10# diesel (%)
N MN DMN TMN	Naphthalene series	60.88	60.90	65.93	33.15	27.95	28.7
B MB DMB TMB	Biphenyl series	2.78	4.91	3.94	14.31	18.73	22.46
A	Acenaphthene series	1.18	0.80	0.33	1.33	3.56	2.84
F MF	Fluorene series	4.16	5.51	2.94	5.70	23.83	22.25
DBT MDBT DMDBT	DBT series	19.21	10.80	9.13	16.85	17.55	13.53
P MP DMP TMP	Phenanthrene series	10.44	15.75	15.36	27.46	8.38	10.22
PY MPY	Pyrene series	0.77	0.75	2.37	1.20	0	0
C	Chrysene series	0.58	0.58	0	0	0	0

[a]Naphthalene (N); methylnaphthalene (MN); dimethylnaphthalene (DMN); trimethylnaphthalene (TMN); biphenyl (B); methylbiphenyl (MB); dimethylbiphenyl (DMB); acenaphthene (A); fluorene (F); methylfluorene (MF); dibenzothiophene (DBT); methyldibenzothiophene (MDBT); dimethyldibenzothiophene (DMDBT); phenanthrene (P); methylphenanthrene (MP); dimethylphenanthrene (DMP); trimethylphenanthrene (TMP); pyrene (PY); methylpyrene (MPY); and chrysene (C).

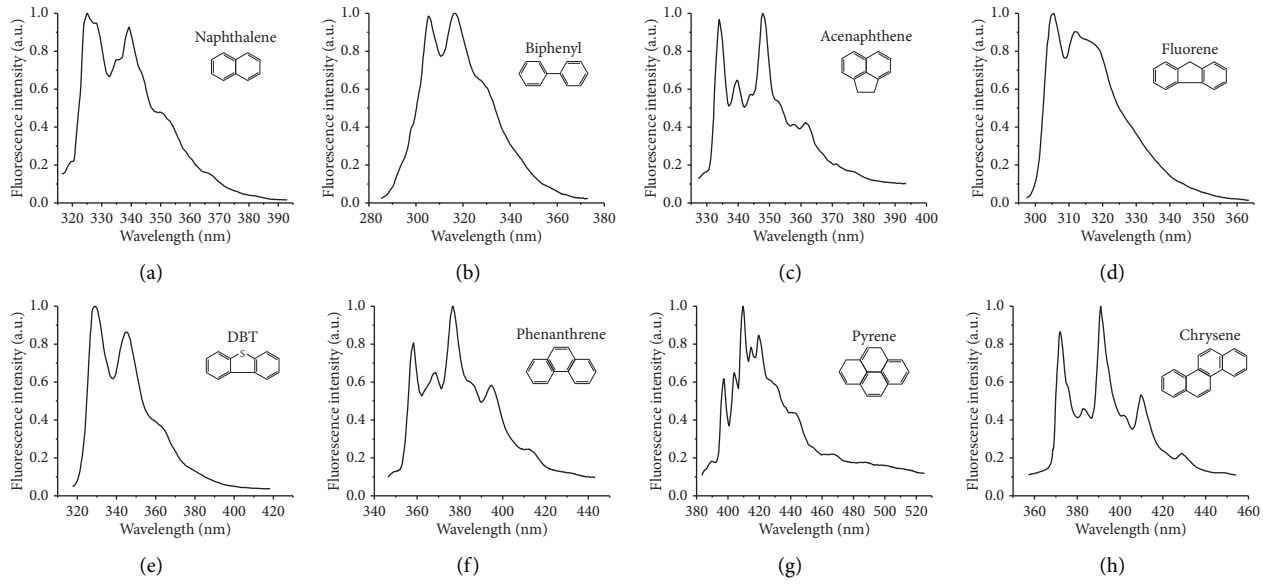

Figure 3: Fluorescence spectra of the individual AHs obtained from the US-EPA.

peaks in the composite fluorescence spectra, especially those of 380# fuel oil at 350–400 nm, could not be detected in the experimental fluorescence spectra (Figure 4(c)). These results were similar to the fluorescence spectral patterns reported in previous studies on oil-contaminated seawater samples [41–43].

These significant differences could be explained considering the effect of heavy petroleum hydrocarbons (high API gravity and viscosity) or the possible interaction between AHs and other aromatic ring systems in the oil samples. In particular, fuel oils, and especially 380# fuel oil, are the heaviest samples among the six oils examined in this study and contain heavy petroleum hydrocarbons (e.g., unidentified AHs, resins, and asphaltenes) with strong fluorescence emission in the long-wavelength range. In contrast, a reduction of the experimental spectra between

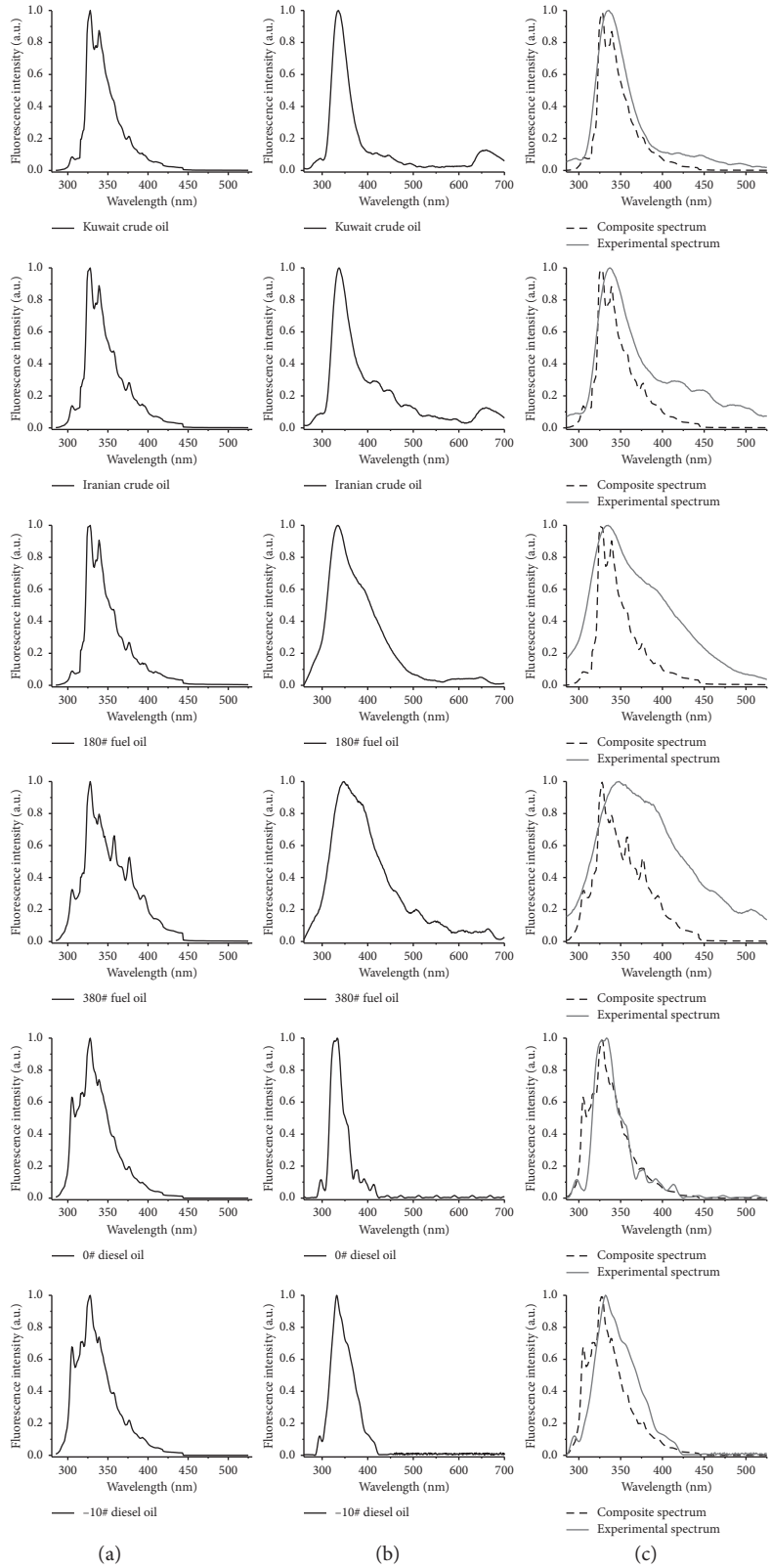

Figure 4: (a) Composite ($\mathbf{X_F} = \mathbf{E}$) and (b) experimental fluorescence spectra (260–700 nm) of Kuwait crude, Iranian crude, 380#, 180# fuel, 0#, and −10# diesel oil samples. (c) Comparison of the composite and experimental fluorescence spectra of the six oil samples between 285 and 525 nm.

300 and 320 nm compared with the composite spectra is evident in diesel oil samples. Therefore, we concluded that, in order to successfully quantify the effect of AHs on the fluorescence spectra of the six oil samples, the differences between the experimental and composite fluorescence spectra and their correlation with the physical properties (API gravity and viscosity) of the oil samples should be first analyzed, as they reflect the content of heavy petroleum hydrocarbons.

3.3. Fluorescence Spectra Difference Analysis. To further analyze the effects of heavy petroleum hydrocarbons on the fluorescence of different oil species in seawater, the differences between the composite and experimental fluorescence spectra were quantified to establish the relationship between the physical parameters and the spectral differences. To that end, we used the redshift of the main peak position (Δf), which was determined by the wavelength of the maximum fluorescence intensity in the experimental and composite fluorescence spectra, and the fluorescence intensity distance (D_F) within the composite and experimental fluorescence spectra [44], which represented the average difference between the composite and experimental spectra and could be calculated as follows:

$$D_F = \frac{1}{n}\sum_{i=1}^{n}\sqrt{(a_i - b_i)^2}, \tag{3}$$

where n is the spectrograph sample number and a_i and b_i are the fluorescence intensities of the composite and experimental spectra, respectively.

In addition, the overall shape similarity between the experimental and composite fluorescence spectra of the six oil samples was analyzed using the spectral angle mapping (SAM) method [45]. SAM is a supervised classification technique that quantifies the angle between the target and the reference spectral vector using spectra as high-dimensional vectors. Small angles indicate high similarity between the two spectra. Moreover, the SAM method was selected, as it uses all the dimensional information of the spectrum, emphasizes its shape characteristics, and reduces the feature information.

In this study, each composite fluorescence spectrum was used as the high-dimensional vector of the reference spectrum, while the experimental fluorescence spectra were used as the high-dimensional vectors of the target spectra. The generalized included angle cosine (θ) of the six oil samples was calculated as follows:

$$\theta = \cos^{-1}\left\{\frac{\sum_{i=1}^{n} t_i r_i}{\sqrt{\left(\sum_{i=1}^{n} t_i^2\right)}\sqrt{\left(\sum_{i=1}^{n} r_i^2\right)}}\right\}, \tag{4}$$

where n is the spectrograph sample number, while $T = (t_1, t_2, \ldots, t_i)$ and $R = (r_1, r_2, \ldots, r_i)$ represent the experimental and composite fluorescence spectra, respectively. The Δf, D_F, and θ values determined for the experimental and composite fluorescence spectra of the six oil samples are summarized in Table 3.

Table 3: Redshift of the main peak position (Δf), fluorescence intensity distance (D_F), and generalized included angle cosine (θ) determined for the experimental and composite fluorescence spectra.

Oil samples	Δf (nm)	D_F (a.u.)	θ (°)
Kuwait crude oil	8	0.079	0.2186
Iranian crude oil	9	0.164	0.3871
180# fuel oil	7	0.258	0.5221
380# fuel oil	20	0.304	0.5003
0# diesel oil	5	0.051	0.3416
−10# diesel oil	4	0.095	0.3970

Correlation analysis was also performed to examine the correlation of the physical properties (API gravity and viscosity) and the spectral difference parameters (Δf, D_F, and θ). In particular, the API gravity was negatively correlated with Δf, D_F, and θ ($R^2 = 0.44$, 0.85, and 0.52, respectively) (Figure 5(a)), while the viscosity showed a positive correlation with Δf, D_F, and θ with R^2 values of 0.74, 0.81, and 0.51, respectively (Figure 5(b)). Based on the API gravity and viscosity data (Table 1), the 380# fuel oil was the heaviest among the six oil samples, as it contained the highest amount of heavy petroleum hydrocarbons. Given also the correlation of the API gravity and viscosity of the six oil samples and their fluorescence spectral difference, we concluded that heavy petroleum hydrocarbons can affect the fluorescence spectra, leading to differences between the experimental and composite fluorescence spectra.

In addition, the fluorescence spectral difference and correlation analysis implied that the six oil samples can be distinguished and identified in the scattered plots. Consequently, fluorescence spectroscopy in combination with GC–MS is an effective strategy to study the effects of heavy petroleum hydrocarbons on the fluorescence spectra of different oil species in seawater and determine the presence of different oil species.

3.4. Contribution of Individual AHs. Considering the AHs relative content information (Section 3.1), the characteristic diagonal matrix ($\mathbf{X_F}$) was constructed to estimate the contribution rate of the eight AH categories (i.e., naphthalene, biphenyl, acenaphthene, fluorene, DBT, phenanthrene, pyrene, and chrysene series) using the fluorescence composition method (equation (5)).

$$\mathbf{X}_F = \frac{\mathbf{I}_{\mathrm{f}}^{\mathrm{oil}}}{\mathbf{I}_f^{\mathrm{AH}}\mathbf{X}_C} = \begin{bmatrix} \omega_{\mathrm{NS}} & 0 & \cdots & 0 \\ 0 & \omega_{\mathrm{BS}} & \cdots & \vdots \\ \vdots & \vdots & \ddots & 0 \\ 0 & \cdots & 0 & \omega_{\mathrm{CS}} \end{bmatrix}_{8\times 8}. \tag{5}$$

The corresponding results (Table 4) confirmed the complex contribution of AHs in the six oil samples. More specifically, it was clear that the AHs of the fluorene series contributed negatively to the experimental fluorescence spectra of all oil samples regardless of their relative content. Moreover, except for 0# diesel oil, the AHs of the

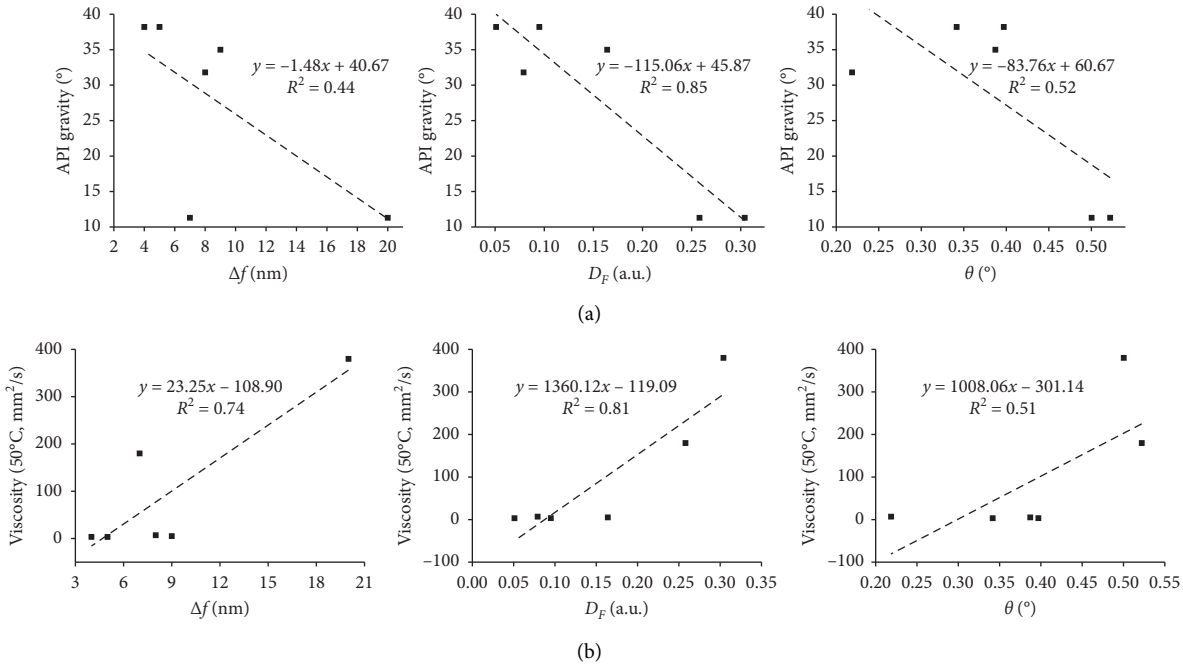

Figure 5: Correlation analysis of the relationship between the (a) API gravity and (b) viscosity of the six oil samples and the main peak position (Δf), fluorescence intensity distance (D_F), and generalized included angle cosine (θ).

Table 4: Contribution of eight AH series in Kuwait crude, Iranian crude, 180# fuel, 380# fuel, 0# diesel, and −10# diesel oil samples.

	Kuwait crude oil	Iranian crude oil	180# fuel oil	380# fuel oil	0# diesel oil	−10# diesel oil
Naphthalene series	1.05	0.96	0.72	0.96	3.5	1.82
Biphenyl series	9.94	6.35	19.13	4.5	2.39	1.52
Acenaphthene series	33.73	61.05	137.86	47.44	2.82	10.64
Fluorene series	−1.39	−1.67	−5.55	−2.91	−0.70	−0.03
DBT series	0.98	1.62	1.43	1.04	−0.67	1.96
Phenanthrene series	1.76	2.31	3.87	3.21	1.06	4.04
Pyrene series	18.48	52.69	17.66	53.48	—	—
Chrysene series	−11.33	−12.75	—	—	—	—

acenaphthene series had the greatest positive contribution to the experimental spectra, while the pyrene series also showed strong positive contribution to the crude and fuel oil samples despite their low individual relative contents. It is worth noting that these AH contributions were particularly obvious in fuel and crude oils, which contain high amounts of heavy petroleum hydrocarbons. In contrast, the contribution of AHs to the fluorescence spectra of diesel oils was more balanced.

Furthermore, it has been reported that UV-induced fluorescence of oils in seawater involves a multidimensional complicated process based on the electronic energy level for the transition of the specific structure of organic matter [46]. The combination of complex composition and multiplicity along with energy transfer and intermolecular interactions can also lead to a very complex pattern of energy levels [47]. In addition, the energy transfer between fluorene and other fluorescing AHs can be explained by the occurrence of an external heavy atom effect in oil samples containing high amounts of heavy petroleum hydrocarbons [16, 48], indicating that AHs affect the fluorescence spectra of oils by quenching signals and generating other peaks. These literature reports further supported our findings that oil samples in seawater can be distinguished based on the fluorescence spectral difference and the contribution of individual AHs. However, this complex effect of external heavy atom required further detailed study on the components of petroleum oils.

4. Conclusion

In this study, a composite method and correlation analyses of fluorescence spectra characteristics and the API gravity and viscosity of the oil samples were carried out. Moreover, we combined the GC-MS and fluorescence analyses to identify and quantify the contribution and effects of eight categories of AHs in oil samples. A detailed database of the AH content of different oil species is needed to apply the composition method we developed. Our study revealed that the effect of heavy petroleum hydrocarbons as well as the relative content of AHs and their potential interactions should be taken into account to sufficiently interpret the

fluorescence spectra of different oil species in seawater. Although the composition method we developed by both fluorescence spectroscopy and GC–MS analysis cannot replace the standard chromatographic techniques, it can be used as a low-cost and efficient screening method for the detection and identification of oil species in seawater. According to the fluorescence spectra characteristics of different oil species, in future, it would help the selection of the characteristic band of the oil spill *via* the fluorescence detection sensor.

Data Availability

The spectral data used to support the findings of this study are available from the corresponding author upon request.

Conflicts of Interest

The authors declare no conflicts of interest.

Acknowledgments

This research was funded by the National Key R&D Program of China (grant no.2020YFE0201500), the National Marine Public Welfare Project (grant no. 201305002), and the Fundamental Research Funds for the Central Universities (grant nos. 3132014302 and 3132019350).

References

[1] M. Fingas and C. E. Brown, "Oil spill remote sensing," in *Earth System Monitoring*, pp. 337–388, Springer, Berlin, Germany, 2013.

[2] E. M. Carstea, C. L. Popa, A. Baker, and J. Bridgeman, "In situ fluorescence measurements of dissolved organic matter: a review," *Ence of the Total. Environment*, vol. 699, 2019.

[3] M. Fingas and C. Brown, "A review of oil spill remote sensing," *Sensors*, vol. 18, no. 2, p. 91, 2017.

[4] C. E. Brown and M. F. Fingas, "Review of the development of laser fluorosensors for oil spill application," *Marine Pollution Bulletin*, vol. 47, no. 9-12, pp. 477–484, 2003.

[5] G. Li, Y. Li, B. Liu, Y. Hou, and J. Fan, "Analysis of scattering properties of continuous slow-release slicks on the sea surface based on polarimetric synthetic aperture radar," *ISPRS International Journal of Geo-Information*, vol. 7, no. 7, p. 237, 2018.

[6] G. Guo, B. Liu, and C. Liu, "Thermal infrared spectral characteristics of bunker fuel oil to determine oil-film thickness and API," *Journal of Marine Science and Engineering*, vol. 8, no. 2, p. 135, 2020.

[7] Y. Li, C. Cui, Z. Liu et al., "Detection and monitoring of oil spills using moderate/high-resolution remote sensing images," *Archives of Environmental Contamination and Toxicology*, vol. 73, no. 1, pp. 154–169, 2017.

[8] E. Baszanowska and Z. Otremba, "Detecting the presence of different types of oil in seawater using a fluorometric index," *Sensors*, vol. 19, no. 17, p. 3774, 2019.

[9] E. Baszanowska and Z. Otremba, "Seawater fluorescence near oil occurrence," *Sustainability*, vol. 12, no. 10, p. 4049, 2020.

[10] F. J. Arques-Orobon, F. Prieto-Castrillo, N. Nuñez, and V. Gonzalez-Posadas, "Processing fluorescence spectra for pollutants detection systems in inland waters," *Sensors*, vol. 20, no. 11, p. 3102, 2020.

[11] T. Hengstermann and R. Reuter, "Laser remote sensing of pollution of the sea: a quantitative approach. European Association of Remote Sensing Laboratories, Advances in," *Remote Sensing*, vol. 1, pp. 52–60, 1992.

[12] J. Han, Y. Liang, B. Zhao, Y. Wang, F. Xing, and L. Qin, "Polycyclic aromatic hydrocarbon (PAHs) geographical distribution in China and their source, risk assessment analysis," *Environmental Pollution*, vol. 251, pp. 312–327, 2019.

[13] Y. Hou, Y. Li, B. Liu, Y. Liu, and T. Wang, "Design and implementation of a coastal-mounted sensor for oil film detection on seawater," *Sensors*, vol. 18, no. 2, p. 70, 2017.

[14] Y. Saito, K. Takano, F. Kobayashi, K. Kobayashi, and H.-D. Park, "Development of a UV laser-induced fluorescence lidar for monitoring blue-green algae in Lake Suwa," *Applied Optics*, vol. 53, no. 30, pp. 7030–7036, 2014.

[15] O. Bukin, D. Proschenko, C. Alexey et al., "New solutions of laser-induced fluorescence for oil pollution monitoring at sea," *Photonics*, vol. 7, no. 2, p. 36, 2020.

[16] Y. V. Fedotov, D. A. Kravtsov, S. L. Belov, and V. A. Gorodnichev, "Experimental studies of efficient sensing fluorescence radiation bands to detect oil and petroleum product spills," *Journal of Physics: Conference Series*, vol. 1399, 2019.

[17] D. Seo, S. Oh, S. Shin, M. Lee, Y. Hwang, and S. Seo, "Smartphone compatible on-site fluorescence analyzer for spilled crude oil based on CMOS image sensor," *Sensors and Actuators B: Chemical*, vol. 289, pp. 93–99, 2019.

[18] W. Jiang, J. Li, X. Yao, E. Forsberg, and S. He, "Fluorescence hyperspectral imaging of oil samples and its quantitative applications in component analysis and thickness estimation," *Sensors*, vol. 18, no. 12, p. 4415, 2018.

[19] M. Jha, J. Levy, and Y. Gao, "Advances in remote sensing for oil spill disaster management: state-of-the-art sensors technology for oil spill surveillance," *Sensors*, vol. 8, no. 1, pp. 236–255, 2008.

[20] D. M. Pampanin and M. O. Sydnes, "Polycyclic aromatic hydrocarbons a constituent of petroleum: presence and influence in the aquatic environment," *Intech Rijeka*, vol. 5, pp. 83–118, 2013.

[21] N. Ferretto, M. Tedetti, C. Guigue, S. Mounier, R. Redon, and M. Goutx, "Identification and quantification of known polycyclic aromatic hydrocarbons and pesticides in complex mixtures using fluorescence excitation-emission matrices and parallel factor analysis," *Chemosphere*, vol. 107, pp. 344–353, 2014.

[22] P. Giamarchi, L. Stephan, S. Salomon, and A. Le Bihan, "Multicomponent determination of a polyaromatic hydrocarbon mixture by direct fluorescence measurements," *Journal of Fluorescence*, vol. 10, no. 4, pp. 393–402, 2000.

[23] S. Retelletti Brogi, B. Charrière, M. Gonnelli et al., "Effect of UV and visible radiation on optical properties of chromophoric dissolved organic matter released by Emiliania huxleyi," *Journal of Marine Science and Engineering*, vol. 8, no. 11, p. 888, 2020.

[24] C. M. Reddy and J. G. Quinn, "GC-MS analysis of total petroleum hydrocarbons and polycyclic aromatic hydrocarbons in seawater samples after the North Cape oil spill," *Marine Pollution Bulletin*, vol. 38, no. 2, pp. 126–135, 1999.

[25] U. H. Yim, S. Y. Ha, J. G. An et al., "Fingerprint and weathering characteristics of stranded oils after the Hebei Spirit oil spill," *Journal of Hazardous Materials*, vol. 197, pp. 60–69, 2011.

[26] M. U. Kumke, H.-G. Löhmannsröben, and T. Roch, "Fluorescence spectroscopy of polynuclear aromatic compounds in environmental monitoring," *Journal of Fluorescence*, vol. 5, no. 2, pp. 139–152, 1995.

[27] S. D. Alaruri, "Multiwavelength laser induced fluorescence (LIF) LIDAR system for remote detection and identification of oil spills," *Optik*, vol. 181, pp. 239–245, 2019.

[28] S. M. Babichenko, A. E. Dudelzak, L. Poryvkina, U. N. Singh, T. Itabe, and Z. Liu, "Quantitative analytical monitoring of aquatic and terrestrial targets with multiwavelength FLS lidars," *Lidar Remote Sensing for Industry & Environment Monitoring III*, vol. 4893, pp. 456–464, 2003.

[29] K. Hyukjoon and Y. Jack, "Polarized reflectance of aluminum and nickel to 532, 355 and 266 nm Nd:YAG laser beams for varying surface finish," *Optics & Laser Technology*, vol. 44, 2012.

[30] Y. Li, Y. Liu, D. Jiang, J. Xu, X. Zhao, and Y. Hou, "Effects of weathering process on the stable carbon isotope compositions of polycyclic aromatic hydrocarbons of fuel oils and crude oils," *Marine Pollution Bulletin*, vol. 133, pp. 852–860, 2018.

[31] Y. Liu, J. Xu, W. Chen, and Y. Li, "Effects of short-term weathering on the stable carbon isotope compositions of crude oils and fuel oils," *Marine Pollution Bulletin*, vol. 119, no. 1, pp. 238–244, 2017.

[32] A. Pandey, A. Yadav, S. Bhawna, and S. Pandey, "Fluorescence quenching of polycyclic aromatic hydrocarbons within deep eutectic solvents and their aqueous mixtures," *Journal of Luminescence*, vol. 183, pp. 494–506, 2017.

[33] B. Apicella, A. Ciajolo, and A. Tregrossi, "Fluorescence spectroscopy of complex aromatic mixtures," *Analytical Chemistry*, vol. 76, no. 7, pp. 2138–2143, 2004.

[34] S. D. Emsbo-Mattingly and E. Litman, *5-Polycyclic Aromatic Hydrocarbon Homolog and Isomer Fingerprinting*, Elsevier, 2016.

[35] B. Nabbefeld, K. Grice, R. E. Summons, L. E. Hays, and C. Cao, "Significance of polycyclic aromatic hydrocarbons (PAHs) in Permian/Triassic boundary sections," *Applied Geochemistry*, vol. 25, no. 9, pp. 1374–1382, 2010.

[36] P. Daling, L.-G. Faksness, A. Hansen, and S. Stout, "Improved and standardized methodology for oil spill fingerprinting," *Environmental Forensics*, vol. 3, no. 3, pp. 263–278, 2002.

[37] S. Stout and Z. Wang, *Standard Handbook Oil Spill Environmental Forensics: Fingerprinting and Source Identification*, pp. 255–312, Academic Press, Cambridge, MA, USA, 2016.

[38] L. E. Brady, "Handbook of fluorescence spectra of aromatic molecules," *Journal of Medicinal Chemistry*, vol. 9, no. 6, p. 984, 1966.

[39] L. Greene, B. Elzey, M. Franklin, and S. O. Fakayode, "Analyses of polycyclic aromatic hydrocarbon (PAH) and chiral-PAH analogues-methyl-β-cyclodextrin guest-host inclusion complexes by fluorescence spectrophotometry and multivariate regression analysis," *Spectrochimica Acta Part A: Molecular and Biomolecular Spectroscopy*, vol. 174, pp. 316–325, 2017.

[40] E. Selli, C. Zaccaria, F. Sena, G. Tomasi, and G. Bidoglio, "Application of multi-way models to the time-resolved fluorescence of polycyclic aromatic hydrocarbons mixtures in water," *Water Research*, vol. 38, pp. 2268–2275, 2004.

[41] Y. Hou, Y. Li, Y. Liu, G. Li, and Z. Zhang, "Effects of polycyclic aromatic hydrocarbons on the UV-induced fluorescence spectra of crude oil films on the sea surface," *Marine Pollution Bulletin*, vol. 146, pp. 977–984, 2019.

[42] E. Baszanowska, Z. Otremba, and J. Piskozub, "Modelling remote sensing reflectance to detect dispersed oil at sea," *Sensors*, vol. 20, no. 3, p. 863, 2020.

[43] F. S. Mirnaghi, N. P. Pinchin, Z. Yang, B. P. Hollebone, P. Lambert, and C. E. Brown, "Monitoring of polycyclic aromatic hydrocarbon contamination at four oil spill sites using fluorescence spectroscopy coupled with parallel factor-principal component analysis," *Environmental Science: Processes & Impacts*, vol. 21, no. 3, pp. 413–426, 2019.

[44] S. Oh, D. Seo, K. Ann et al., "Oil fluorescence spectrum analysis for the design of fluorimeter," *Journal of the Korean Society for Marine Environment & Energy*, vol. 18, no. 4, pp. 304–309, 2015.

[45] J. H. Christensen, A. B. Hansen, J. Mortensen, and O. Andersen, "Characterization and matching of oil samples using fluorescence spectroscopy and parallel factor analysis," *Analytical Chemistry*, vol. 77, no. 7, pp. 2210–2217, 2005.

[46] A. K. Sarma and A. G. Ryder, "Comparison of the fluorescence behavior of a biocrude oil and crude petroleum oils," *Energy & Fuels*, vol. 20, no. 2, pp. 783–785, 2006.

[47] Y. Cai, Y. Zou, C. Liang, and B. Zou, "Research on polarization of oil spill and detection," *Acta Oceanologica Sinica*, vol. 35, no. 3, pp. 84–89, 2016.

[48] R. L. Joseph, *Principles of Fluorescence Spectroscopy*, Plenum Press, Baltimore, MD, USA, 1983.